

## FLOW BEHAVIOUR OF GLYCOLATED WATER SUSPENSIONS OF FUNCTIONALIZED GRAPHENE NANOPATELETS

Gómez-Barreiro S.<sup>1</sup>, Vallejo J. P.<sup>1,3</sup>, Cabaleiro D.<sup>1</sup>, Gracia-Fernández C.<sup>2</sup>, Fernández-Seara J.<sup>3</sup>, Lugo L.<sup>1\*</sup>

<sup>1</sup> Departamento de Física Aplicada, Facultade de Ciencias  
Universidade de Vigo  
Vigo, 36310, Spain

<sup>2</sup> TA Instruments-Waters LLC  
New Castle, DE 19720, USA

<sup>3</sup> Área de Máquinas y Motores Térmicos, Escola de Enxeñaría Industrial  
Universidade de Vigo  
Vigo, 36310, Spain

E-mail: luis.lugo@uvigo.es

### ABSTRACT

The heat transfer performance of the conventional fluids used in heat exchange processes improves by dispersing nanoparticles with high thermal conductivity, as many researches have shown in the last decades. The heat transfer capability of a fluid depends on several physical properties among which the rheological behavior is very relevant, as we have previously pointed out.

In this study, different samples of nanofluids have been analyzed by using a DHR-2 rotational rheometer of TA Instruments with concentric cylinder geometry in the temperature range from (278.15 to 323.15) K. The used base fluids were two different binary mixtures of propylene glycol and water at (10:90)% and (30:70)% mass ratios. Two different mass concentrations (viz. 0.25 and 0.5 wt.%) of graphene nanoplatelets functionalized with sulfonic acid (graphenit-HW6) were dispersed in these two base fluids.

Firstly, with the goal of checking and calibrating the operation of the rheometer, the viscosity-shear stress curves for pure propylene glycol, Krytox GPL102 oil, and the two base fluids were experimentally determined. A detailed comparative study with those well-known data over the entire range of temperature was stabilized obtaining deviations in viscosity less than 3.5%. Then, the flow curves of the different nanofluid samples were studied at different temperatures to characterize their flow behavior.

### INTRODUCTION

The enhancement of the heat transfer performance has raised great interest during the last century since an increment in the efficiency of thermal facilities could lead to huge savings in their initial and operational costs [1]. Once different approaches such as the use of extended surfaces or the optimization of flow conditions have been extensively investigated, many researchers focus on improving the weak thermal capabilities of most conventional working fluids. A promising way to achieve this aim is by dispersing nano-sized particles with high thermal conductivity in these conventional heat transfer fluids (HTFs). These new nanostructured materials

are known as nanofluids and exhibit clear advantages regarding the dispersions of millimeter or micrometer particles such as lower pressure drops or clogging issues [2-3].

Among the different nanoadditives used to design new nanofluids in the past decade, carbon allotropes seem to be those with the most remarkable potential [4]. Within the graphite family, the exceptional mechanical, thermal and electrical properties of graphene (ideally envisaged as a single-atom-thick sheet of hexagonally arranged, sp<sup>2</sup>-bonded carbon atoms tightly packed into a honeycomb lattice) has attracted great attention since this structure was experimentally isolated by Novoselov et al. [5]. Graphene is commercially available in the form of some-layer stacks (normally between 10-100 layers) known as graphene nanoplatelets which combine the properties of single-layer graphene as well as the possibility of being easily and cost-effectively synthesized. Nevertheless, graphene is hydrophobic and it is not possible to obtain dispersions in water for a long time [6-7]. In the case of graphene oxides (GONPs), their basal planes and sheet edges contain different functional groups and as a consequence the material becomes hydrophilic. The drawback is that the thermal conductivity of graphene oxide is considerably lower than that of pristine graphene since the oxidation process destroys the systematically arranged conjugated structure. Through a reduction of exfoliated graphene oxide, it is possible both to restore the properties of graphene and maintain dispersibility [7].

Different works have shown that the dispersion of nanoparticles remarkably increases the thermal conductivity of conventional HTFs which may lead to improve the heat transfer performance. However, it must also be considered that the addition of nanomaterials can also alter other thermo-physical properties which, in turn, can sometimes offset the thermal conductivity enhancements. Thus, the viscosity (a fundamental property in the Reynolds number) has a strong influence on the flow regime and, consequently, on the heat transfer, for instance. Additionally, an increase in this property can lead to higher pressure drops and, therefore, higher pumping powers [8]. The Newtonian or non-Newtonian nature of the nanofluids

is also a key issue to define the flow type. In addition to study the flow behavior and assess the penalty in pressure drop, the rheological properties of nanofluids are also helpful to analyze the nanoparticle structuring within the dispersions [8-10].

The rheological properties of graphene nanofluids based on water (W) [7, 11-13] or ethylene glycol (EG) [14] have already been studied in the literature. However, up to our knowledge, no research was developed using binary mixtures of propylene glycol and water. In this study, the flow behavior of two graphene nanoplatelet nanofluid sets has been analyzed in the temperature range from (278.15 to 323.15) K by using a DHR-2 rotational rheometer (TA instruments; DE, USA) equipped with concentric cylinder geometry. The nanofluids were designed using two different (propylene glycol + water) mixtures at (10:90)% and (30:70)% mass ratios as base fluids and two mass fractions ( $\varphi = 0.0025$  and  $\varphi = 0.005$ ) of graphene nanoplatelets stabilized with sulfonic acid (graphenit-HW6).

## NOMENCLATURE

<i>AAD</i>		Absolute Average Deviation
<i>A, B</i>		Adjustable parameters in equation (2)
<i>GOnP</i>		Graphene oxide nanoplatelet
<i>PG</i>		Propylene glycol
<i>T</i>	[K]	Temperature
$\eta_0, C, T_0$		Adjustable parameters of Vogel-Fulcher-Tamman (VFT) model, equation (1)
<i>W</i>		Water
Special characters		
$\eta$	[mPa·s]	Dynamic viscosity
$\varphi$	[-]	Graphene oxide nanoplatelet mass fraction
Subscripts		
<i>bf</i>		Base fluid
<i>nf</i>		Nanofluid
<i>np</i>		Nanoparticle

## EXPERIMENTAL

### Materials and sample preparation

Sulfonic acid-functionalized graphene nanoplatelets (graphenit-HW6) were provided by NanoInnova Technologies S.L. (Madrid, Spain, [www.nanoinnova.com](http://www.nanoinnova.com)). The base fluids are two (propylene glycol + water) mixtures at (10:90)% and (30:70)% mass ratios. Propylene glycol was purchased from Sigma-Aldrich with a mass purity of 99.5%, while Milli-Q Grade water was produced with 18.2 M $\Omega$ ·cm at 298.15 K by means of a Milli-Q 185 Plus system (Millipore Ltd, Watford, UK). Nanofluids were designed following a two-step method. Therefore, the amounts of powder and base fluid necessary to obtain the desired nanoparticle mass concentrations (0.25 and 0.5 wt.%) were first weighted in a Sartorius electronic balance model CPA225 (Sartorius AG, Germany) and then stirred at 1500 rpm for 60 minutes. Afterwards, samples were sonicated for 240 minutes by using an ultrasonic bath (Ultrasounds, JP Selecta S.A., Spain) working with a maximum sonication power of 200 W and a frequency of 20 kHz.

## Experimental methods

The shear rate dependence of viscosity, the so-called flow curve, was studied at six different temperatures ranging from (278.15 to 323.15) K by means of a combined motor-transducer Discovery Hybrid Rheometer (DHR-2, TA instruments). This instrument was equipped with a coaxial cylinder geometry consisting of an external cup (diameter: 30.37 mm) and a double gap rotor (bob diameter: 27.98 mm, length: 42.17 mm, and operating gap: 5912.87  $\mu\text{m}$ ) which is appropriate to prevent evaporation of the sample at high temperatures. Sample temperature was controlled by using a Peltier jacket and an equilibration time of at least 20 minutes was waited before experiments in order to ensure a uniform initial temperature. Tests were performed in steady-state regime at shear rates logarithmically increasing from (0.1 to 100)  $\text{s}^{-1}$  with at least five points per decade. With the aim of checking and calibrating the operation of the rheometer, the viscosity-shear stress curves were also determined for Krytox GPL 102 oil and pure propylene glycol over the entire temperature range. A detailed comparative between the experimental viscosities here obtained and values previously reported in the literature [10, 15-20] for these materials is presented in Figure 1.

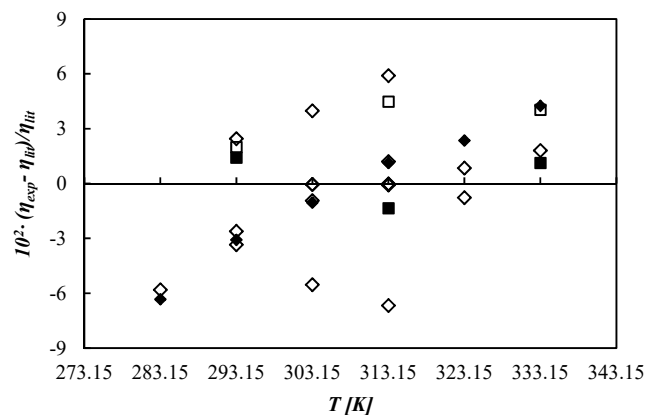


**Figure 1** Comparison between experimental and literature viscosities at different temperatures for: (◆) Krytox GPL 102 oil [16, 21], (◇) propylene glycol, PG, [10, 15, 17-18, 20], (■) PG+W mixture at (10:90)% [22] and (□) PG+W at (30:70)% [22].

The relative deviations and average absolute deviations are lower than 3%.

## RESULTS AND DISCUSSION

The rheological behavior of the two base fluids and the four designed nanofluids was analyzed at temperatures ranging from (278.15 to 323.15) K. As an example, Figure 2 shows viscosity vs. shear rate for the 0.25 wt.% GOnPs (PG+W at 30:70 wt.%) nanofluid at five temperatures whereas Figure 3 shows the viscosity vs. shear rate dependences for the different samples at 293.15 K.

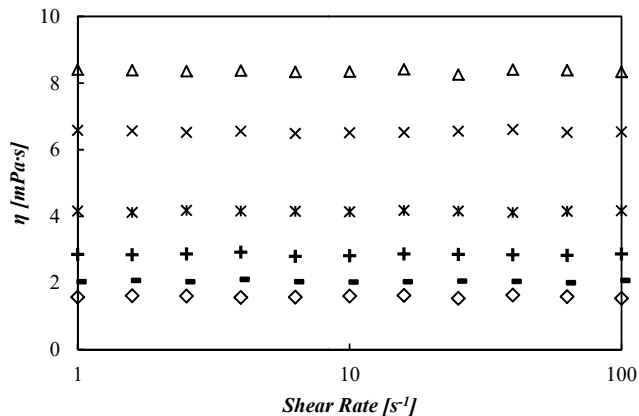


**Figure 2** Flow curve for 0.25 wt.% GONPs (PG+W at 30:70 wt.%) nanofluid at ( $\Delta$ ) 278.15 K, ( $\times$ ) 283.15 K, ( $*$ ) 293.15 K, ( $+$ ) 303.15 K, ( $-$ ) 313.15 K and ( $\diamond$ ) 323.15 K.

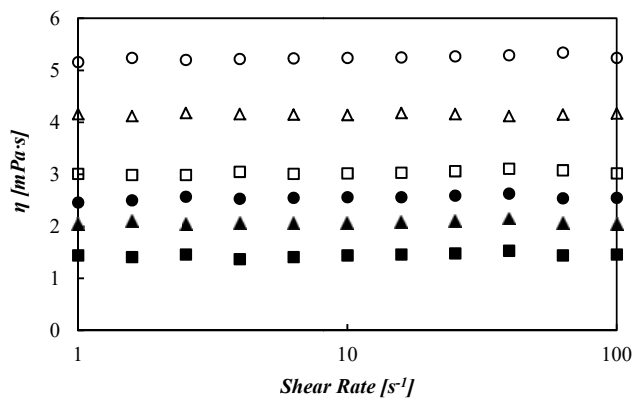


**Figure 3** Flow curve at 293.15 K for: ( $\blacksquare, \blacktriangle, \bullet$ ) (PG+W at 10:90 wt.%) and ( $\square, \triangle, \circ$ ) (PG+W at 30:70 wt.%) nanofluids sets. ( $\blacksquare, \square$ ) Base fluid, 0 wt.%, ( $\blacktriangle, \triangle$ ) 0.25% and ( $\bullet, \circ$ ) 0.5% mass concentrations/wt%.

As it can be observed, both base fluids exhibit a Newtonian behavior overall the analyzed concentration, temperature and shear rate ranges. Our experimental results for the two base fluids were also compared with previous literature data [22]. Absolute average deviations lower than 1.3% and 3.5% were found for the (propylene glycol + water) mixture at (10:90)% and (30:70)% mass ratios, respectively. This good agreement between literature and our measured data for the used base fluids is also shown in Figure 1.

Similarly, both nanofluid sets a Newtonian behavior at the analyzed low concentrations present. The viscosity of the nanofluids and base fluids is strongly dependent on temperature. The increment of the temperature causes that the nanoparticles are motivated more and create more space for them because the weakening of the inter-particles and intermolecular adhesion forces. Figures 4 and 5 show these temperature dependences of the dynamic viscosities obtained for the GONPs nanofluid sets based on (PG+W) mixtures at (10:90)% and (30:70)% mass ratios.

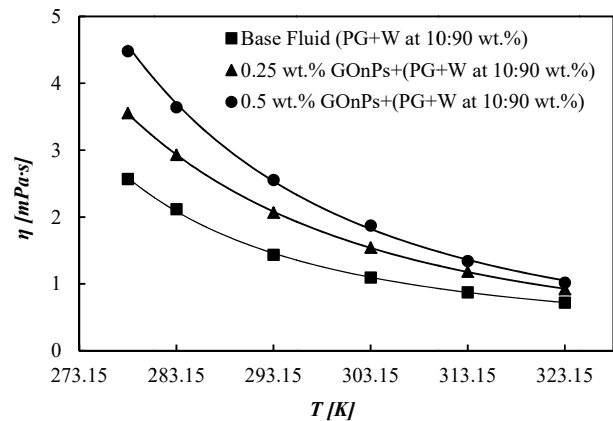


**Figure 4** Temperature dependence of dynamic viscosity of GONPs in (PG+W) at (10:90) wt.%. (—) VFT equation.

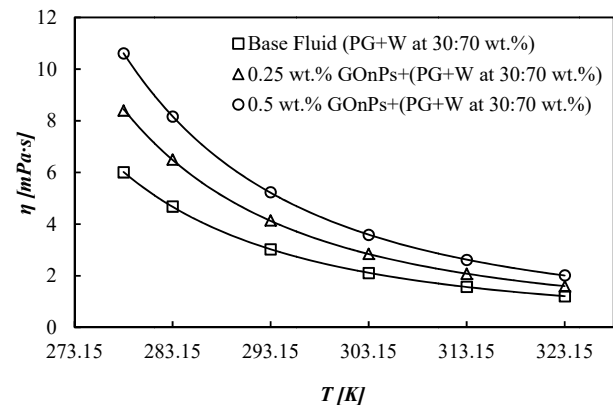


**Figure 5** Temperature dependence of dynamic viscosity of GONPs in (PG+W) at (30:70) wt.%. (—) VFT equation.

The reported decreases in dynamic viscosity with the temperature reach up to 80% which is in agreement to that reported by Sadeghinezhad et al. [23] for aqueous graphene nanoplatelet nanofluids. One of the most used expressions to correlate the temperature dependence of viscosity is the modification of Andrade's equation known as Vogel-Fulcher-Tamman (VFT):

$$\ln \eta(T) = \ln \eta_0 + \frac{C T_0}{T - T_0} \quad (1)$$

where  $\eta_0$ ,  $C$ , and  $T_0$  are the adjustable parameters. The values of these three fitting parameters are gathered for the two studied nanofluid sets in Table 1. VFT equations provides a good description of the temperature dependence, with  $AADs\%$  lower than 1.7%, as it can also be observed in Figures 4 and 5.

**Table 1**  $\eta_0$ ,  $C$ , and  $T_0$  coefficients as well as  $AADs\%$  and standards deviations from Vogel-Fulcher-Tammann (VFT) correlation, equation (1), for the two studied nanofluid sets.

	Base Fluid (0 wt.%)	0.25 wt.%	0.5 wt.%
<i>GONPs/(PG+W at 10:90 wt.%)</i>			
$\eta_0$ [mPa·s]	0.0948	0.0141	0.0134
$C$	236.62	777.46	778.19
$T_0$ [K]	1.145	5.651	5.382
$AADs\%$	0.74	0.36	1.7
$s$ [mPa·s]	0.03	0.01	0.07
<i>GONPs/(PG+W at 30:70 wt.%)</i>			
$\eta_0$ [mPa·s]	0.0493	0.0618	0.0684
$C$	431.78	431.95	461.22
$T_0$ [K]	2.293	2.269	2.470
$AADs\%$	0.20	0.43	0.27
$s$ [mPa·s]	0.008	0.04	0.02

On the other hand, the loading of the graphene oxide nanoplatelets increases the friction and flowing resistance of fluids leading to a viscosity increment. These increases of the dynamic viscosity in relation to base fluids, i.e.  $(\eta_{nf}-\eta_{bf})/\eta_{bf}$ , as a function of the temperature are shown for the two concentrations of GONPs in (PG+W) at (10:90)% and (PG+W) at (30:70)% mass ratios in Figure 6 and Figure 7, respectively.

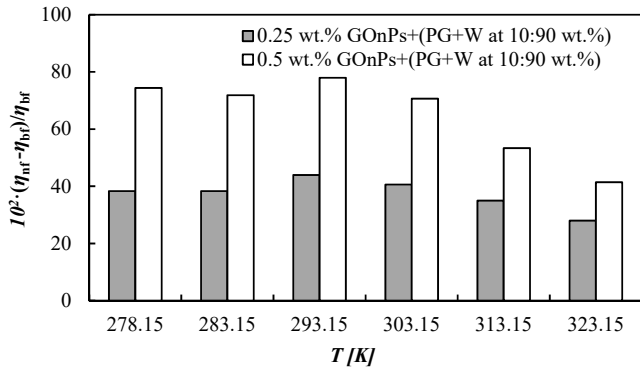


**Figure 6** Dynamic viscosity increases of GONPs in (PG+W) at (10:90)% mass ratio.

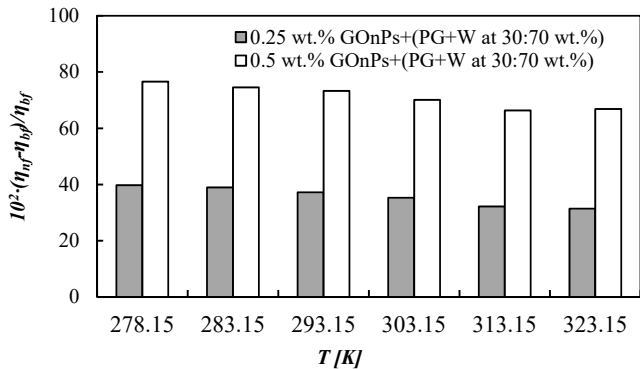


**Figure 7** Dynamic viscosity increases of GONPs in (PG+W) at (30:70)% mass ratio.

As it can be observed, maximum viscosity increases reach up to 44% and 78% at the 0.25% and 0.5% mass concentrations, respectively. Furthermore, the rises in viscosity due to the loading of GONPs show a downward trend with the increasing temperature. This trend can be due to the fact that the surface charge density rises when the temperature increases. In order to detail the effect of the loading of GONPs within the analyzed nanoparticle concentration range, in Figure 8 the  $\eta(\phi)$  curves are shown at the different temperatures for the 10:90 wt.% nanofluids, as an example.

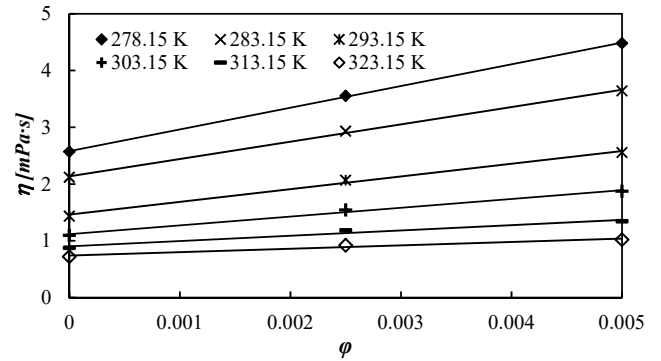


**Figure 8** Concentration dependence of the dynamic viscosity of GONPs/(PG+W at 10:90 wt.%). (—) equation (2).

This concentration dependence is also similar to that exhibited by the studied GONPs/(PG+W 30:70 wt.%) nanofluids. The slopes of the linear fits of GONPs/(PG+W 10:90 wt.%) and GONPs/(PG+W 30:70 wt.%) are gathered in Figure 9.

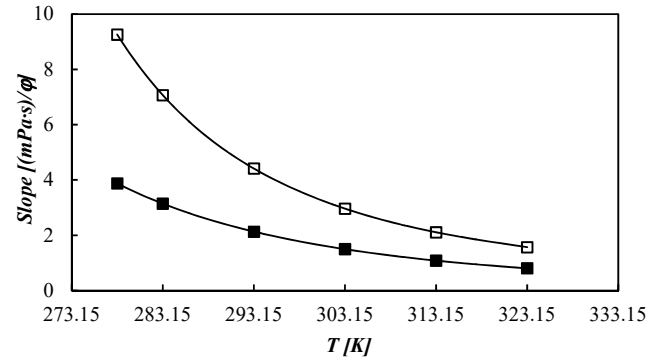


**Figure 9** Slope of the linear  $\eta(\phi)$  curves against temperature: (■) GONPs/(PG+W at 10:90 wt.%) and (□) GONPs/(PG+W at 30:70 wt.%).

As shown in Figure 9, both slope values present exponential dependences with temperature. The nanofluid set based on (PG+W at 30:70%) exhibits slopes twice as high as those of the GONPs/(PG+W at 10:90%) nanofluids within the analyzed temperature range.

The temperature and concentration dependences of the two types of studied nanofluids can be described by using the following equation, proposed in this work:

$$\eta = A e^{\frac{B}{T}} \cdot \phi + \eta_0 e^{\frac{CT_0}{T-T_0}} \quad (2)$$

where  $\varphi$  is the nanoparticle mass fraction,  $T$  is the temperature in K, and  $A$  and  $B$  are the fitting parameters.  $\eta_0$ ,  $C$  and  $T_0$  parameters were taken from Table 1. The obtained coefficients by using this expression for each nanofluid set together with the  $AADs\%$  and standard deviations are gathered in Table 2.

**Table 2**  $A$  and  $B$  coefficients as well as  $AADs\%$  from equation (2) for the two studied nanofluids sets.

Parameters	Nanofluid set	
	GONPs/(PG+W 10:90 wt.%)	GONPs/(PG+W 30:70 wt.%)
$A$ [mPa·s]	0.0040	0.0012
$B$ [K]	3190.83	3764.03
$AADs\%$	2.0	0.92
$s$ [mPa·s]	0.05	0.06

Figure 8 shows the goodness of this equation correlating the  $\eta(\varphi, T)$  curves of both nanofluid sets. The new equation allows describing the viscosity behavior of the analyzed glycolated water suspensions of functionalized graphene nanoplatelets with similar deviations to that provided by the well-known Vogel-Fulcher-Tamman equation. Moreover, it is noteworthy that five fitting parameters are necessary for each nanofluid set by the proposed equation while nine are needed when using VFT.

## CONCLUSIONS

A DHR-2 rotational rheometer of TA Instruments with concentric cylinder geometry was checked in detail in order to determine the flow behavior in a wide temperature and shear rate range. Good agreements were found between our experimental viscosity values for the Newtonian fluids propylene glycol, Kryptox GLP 102 oil, propylene glycol + water mixture at (10:90)% and propylene glycol + water at (30:70)% in the temperature range from (278.15 to 333.15) K and those previously published in the literature. The rheological behavior of two types of glycolated water suspensions of functionalized graphene nanoplatelets has been explored by using the mentioned device at nanoadditive concentrations up to  $\varphi = 0.005$  in mass.

The two sets of nanofluids show a Newtonian behavior overall the analyzed concentration and temperature ranges at shear rates up to  $100 \text{ s}^{-1}$ . For all analyzed nanofluids the diminutions in dynamic viscosity with increasing temperature reach up to 80%. The loading of the graphene oxide nanoplatelets linearly increases the viscosity and these worsening in relation to the base fluid range from (28 to 44)% and from (41 to 78)% for  $\varphi = 0.0025$  and  $0.005$ , respectively. A relationship between viscosity, nanoadditive concentration and temperature is proposed in this work which allows describing the  $\eta(\varphi, T)$  functions with deviations less than  $0.07 \text{ mPa}\cdot\text{s}$  which are similar to those exhibited by  $\eta(T)$  curves employing VFT equation.

## ACKNOWLEDGEMENTS

Authors acknowledge the functionalized graphene nanoplatelets powder provided by Nanoinnova Technologies S.L. (<http://www.nanoinnova.com/Product>). This work was supported by the Ministerio de Economía y Competitividad (Spain) and the FEDER program through the ENE2014-55489-C2-2-R Project. J.P.V. and D.C. acknowledge the financial support under the FPI and FPU Programs by the “Ministerio de Educación, Cultura y Deporte” (Spain), respectively.

## REFERENCES

- [1] Yarmand, H.; Gharekhani, S.; Ahmadi, G.; Shirazi, S. F. S.; Baradaran, S.; Montazer, E.; Zubir, M. N. M.; Alehashem, M. S.; Kazi, S. N.; Dahari, M., Graphene nanoplatelets-silver hybrid nanofluids for enhanced heat transfer, *Energy Conversion and Management*, Vol. 100, 2015, pp. 419-428.
- [2] Mehrali, M.; Sadeghinezhad, E.; Rosen, M. A.; Tahan Latibari, S.; Metselaar, H. S. C.; Kazi, S. N., Effect of specific surface area on convective heat transfer of graphene nanoplatelet aqueous nanofluids, *Experimental Thermal and Fluid Science*, Vol. 68, 2015, pp. 100-108.
- [3] Vajjha, R. S.; Das, D. K., A review and analysis on influence of temperature and concentration of nanofluids on thermophysical properties, heat transfer and pumping power, *International Journal of Heat and Mass Transfer*, Vol. 55, 2012, pp. 4063-4078.
- [4] Park, E. J.; Park, S. D.; Bang, I. C.; Park, Y. B.; Park, H. W., Critical heat flux characteristics of nanofluids based on exfoliated graphite nanoplatelets (xGnPs), *Materials Letters*, Vol. 81, 2012, pp. 193-197.
- [5] Novoselov, K. S.; Geim, A. K.; Morozov, S. V.; Jiang, D.; Zhang, Y.; Dubonos, S. V.; Grigorieva, I. V.; Firsov, A. A., Electric field in atomically thin carbon films, *Science*, Vol. 306, 2004, pp. 666-669.
- [6] Li, X.; Chen, Y.; Mo, S.; Jia, L.; Shao, X., Effect of surface modification on the stability and thermal conductivity of water-based  $\text{SiO}_2$ -coated graphene nanofluid, *Thermochimica Acta*, Vol. 595, 2014, pp. 6-10.
- [7] Mohd Zubir, M. N.; Badarudin, A.; Kazi, S. N.; Huang, N. M.; Misran, M.; Sadeghinezhad, E.; Mehrali, M.; Yusoff, N., Highly dispersed reduced graphene oxide and its hybrid complexes as effective additives for improving thermophysical property of heat transfer fluid, *International Journal of Heat and Mass Transfer*, Vol. 87, 2015, pp. 284-294.
- [8] Azmi, W. H.; Sharma, K. V.; Mamat, R.; Najafi, G.; Mohamad, M. S., The enhancement of effective thermal conductivity and effective dynamic viscosity of nanofluids – A review, *Renewable and Sustainable Energy Reviews*, Vol. 53, 2016, pp. 1046-1058.
- [9] Cabaleiro, D.; Pastoriza-Gallego, M. J.; Gracia-Fernández, C.; Piñero, M. M.; Lugo, L., Rheological and volumetric properties of  $\text{TiO}_2$ -ethylene glycol nanofluids, *Nanoscale Research Letters*, Vol. 8, 2013.
- [10] Calvo-Bravo, J.; Cabaleiro, D.; Piñero, M. M.; Lugo, L., Magnetorheological behaviour of propylene glycol-based hematite nanofluids, *Rheologica Acta*, Vol. 54, 2015, pp. 757-769.
- [11] Amiri, A.; Sadri, R.; Shanbedi, M.; Ahmadi, G.; Chew, B. T.; Kazi, S. N.; Dahari, M., Performance dependence of thermosyphon on the functionalization approaches: An experimental study on thermophysical properties of graphene nanoplatelet-based water nanofluids, *Energy Conversion and Management*, Vol. 92, 2015, pp. 322-330.
- [12] Mehrali, M.; Sadeghinezhad, E.; Latibari, S.; Kazi, S.; Mehrali, M.; Zubir, M. N. B. M.; Metselaar, H. S., Investigation of thermal conductivity and rheological properties of nanofluids containing graphene nanoplatelets, *Nanoscale Research Letters*, Vol. 9, 2014, pp. 15.

- [13] Tesfai, W.; Singh, P.; Shatilla, Y.; Iqbal, M. Z.; Abdala, A. A., Rheology and microstructure of dilute graphene oxide suspension, *Journal of Nanoparticle Research*, Vol. 15, 2013, pp. 1989.
- [14] Hadadian, M.; Goharshadi, E. K.; Youssefi, A., Electrical conductivity, thermal conductivity, and rheological properties of graphene oxide-based nanofluids, *Journal of Nanoparticle Research*, Vol. 16, 2014, pp. 2788.
- [15] ASHRAE Handbook Fundamentals, Physical Properties of Secondary Coolants, Atlanta, Vol. 2009.
- [16] Comuñas, M. J. P.; Gaciño, F. M.; Cabaleiro, D.; Lugo, L.; Fernández, J., Krytox GPL102 oil as reference fluid for high viscosities: High pressure volumetric properties, heat capacities, and thermal conductivities, *Journal of Chemical and Engineering Data*, Vol. 60, 2015, pp. 3660-3669.
- [17] George, J.; Sastry, N. V., Densities, Dynamic Viscosities, Speeds of Sound, and Relative Permittivities for Water + Alkanediols (Propane-1,2- and -1,3-diol and Butane-1,2-, -1,3-, -1,4-, and -2,3-Diol) at Different Temperatures, *Journal of Chemical & Engineering Data*, Vol. 48, 2003, pp. 1529-1539.
- [18] Kapadi, U. R.; Hundiwale, D. G.; Patil, N. B.; Lande, M. K.; Patil, P. R., Studies of viscosity and excess molar volume of binary mixtures of propane-1,2 diol with water at various temperatures, *Fluid Phase Equilibria*, Vol. 192, 2001, pp. 63-70.
- [19] Lemmon, E. W.; Huber, M. L.; McLinden, M. O., NIST Standard Reference Database 23, in: *Reference Fluid Thermodynamic and Transport Properties (REFPROP)*, National Institute of Standards and Technology, Vol. 2010.
- [20] Saleh, M. A.; Habibullah, M.; Shamsuddin Ahmed, M.; Ashraf Uddin, M.; Uddin, S. M. H.; Afsar Uddin, M.; Khan, F. M., Excess molar volumes and viscosities of some alkanols with cumene, *Physics and Chemistry of Liquids*, Vol. 44, 2006, pp. 31-43.
- [21] Harris, K. R., Temperature and Pressure Dependence of the Viscosities of Krytox GPL102 Oil and Di(pentaerythritol) Hexa(isononanoate), *Journal of Chemical & Engineering Data*, Vol. 60, 2015, pp. 1510-1519.
- [22] Melinder, A., Properties of secondary working fluids for indirect systems, *International Institute of Refrigeration (IIR)*, Paris, France, 2010
- [23] Sadeghinezhad, E.; Mehrali, M.; Tahan Latibari, S.; Kazi, S. N.; Oon, C. S.; Metselaar, H. S. C., Experimental investigation of convective heat transfer using graphene nanoplatelet based nanofluids under turbulent flow conditions, *Industrial and Engineering Chemistry Research*, Vol. 53, 2014, pp. 12455-12465.